Rothfuss, N. E., Marsh, A., Rovelli, G., Petters, M. D., & Reid, J. P. (2018). Condensation Kinetics of Water on Amorphous Aerosol Particles. *Journal of Physical Chemistry Letters*, *9*(13), 3708-3713. https://doi.org/10.1021/acs.jpclett.8b01365

The Condensation Kinetics of Water on Amorphous Aerosol Particles

Nicholas E. Rothfuss,[1] Aleksandra Marsh,[2] Grazia Rovelli,[2] Markus D. Petters,[1] Jonathan P. Reid[2]*

[1] Department of Marine, Earth, and Atmospheric Sciences, North Carolina State University, Raleigh, NC, USA 27695

[2] School of Chemistry, University of Bristol, Bristol, UK, BS8 1TS

Corresponding Author

*E-mail: j.p.reid@bristol.ac.uk, Tel: +44 117 331 7388.

ABSTRACT.

Responding to changes in the surrounding environment, aerosol particles can grow by water condensation changing rapidly in composition and changing dramatically in viscosity. The timescale for growth is important to establish for particles undergoing hydration processes in the atmosphere or during inhalation. Using an electrodynamic balance, we report direct measurements at -7.5, 0 and 20 ºC of timescales for hygroscopic condensational growth on a range of model hygroscopic aerosol systems. These extend from viscous aerosol particles containing a single saccharide solute (sucrose, glucose, raffinose or trehalose) and a starting viscosity equivalent to a glass of ~10^{12} Pas, to non-viscous (~10^{-2} Pa·s) tetraethylene glycol particles. The condensation timescales observed in this work indicate water condensation occurs rapidly at all temperatures

examined (< 10 s) and for particles of all initial viscosities spanning 10^{-2} to 10^{12} Pa·s. Only a marginal delay (<1 order of magnitude) is observed for particles starting as a glass.

TOC GRAPHICS

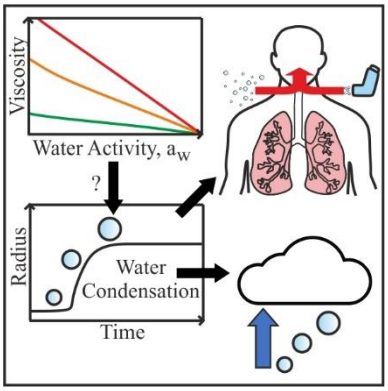

Quantifying the rate of condensation of water on aerosol particles is important for a diverse set of problems, including predicting cloud droplet number concentration in the atmosphere and understanding the size dynamics and deposition profile of particles on inhalation to the respiratory tract.[1] Conversely, understanding the coupling between mass and heat transport during evaporation is central to modelling the performance of sprays in a range of applications and the production of functionalized particles by spray drying.[2,3] In many of these contexts, particles are >>1 μm in diameter (or grow above this size) and the process occurs at ambient pressure. Under these conditions the particle hygroscopic growth rate is limited by the rate at which mass is moved towards or away from the particle surface in the gas phase, rather than molecular exchange at the surface or diffusion within the particle bulk. Such behavior is particularly likely if the particle is a liquid droplet. However, when the particle is crystalline or amorphous, the possible impact of dissolution kinetics or slow diffusion within the particle bulk on the rate of condensation and evaporation must be considered. In such cases, timescales of bulk or interfacial transport may be

longer than those of gas diffusion.[4–6] Alternatively, dissolution resulting from water uptake may remove bulk diffusional limitations present in the dry, solid-like phase.[7] Organic particles (OA) can exist as viscous semi-solid[8–15] or amorphous solid (glassy) phases.[16–19] For a hygroscopic particle starting as an amorphous solid, the condensation of water often leads to a decrease in particle viscosity, particularly if the particle must progress from a glass (10^{12} Pa·s)[20] to a dilute solution droplet (10^{-3} Pa·s), which can happen at very high relative humidities (RH) observed during cloud droplet formation or inhalation. Although the evaporation and condensation kinetics of water in highly viscous aerosol particles can be limited by slow diffusion of water within a particle, particularly at low RH [21,22] the impact of a viscous core on condensation kinetics at high RH remains uncertain. Addressing this uncertainty is the focus of this paper.

Continuous water condensation is often observed for hygroscopic amorphous particles as the RH is increased instead of the sharp, solubility-dependent deliquescence phase transition observed for crystalline particles.[23–25] The anticipated equilibration time for a low viscosity submicron particle following an RH change is <<1 s, increasing to >10 s for a 10 μm particle diameter.[8] For highly viscous semi-solid and glassy solid particles, the equilibration timescale may be much longer. At a microscopic level, a particle undergoing water uptake can be viewed as a series of concentric shells of varying viscosity/diffusivity.[26,27] While it is reasonable to expect that the outermost shells will readily equilibrate with the surrounding RH, even for highly viscous particles, absorbed water vapor may not readily penetrate into the particle interior if bulk diffusivity is sufficiently low.[21] Condensational growth will be complete when an equilibrium exists between the water activity of the particle and gas phase. According to the Stokes-Einstein relation, the diffusivity of a molecule within a matrix is inversely proportional to the viscosity. Although the Stokes-Einstein relationship is known to fail in matrices of semi-solid viscosity[10,28–

[32] and the divergence is most drastic for small molecules like water, as a first estimate it would suggest that the diffusivity within a glassy particle could be as much as 12 orders of magnitude less than observed within a particle of liquid-like nature.[9] If bulk diffusional limitations are present, water uptake may happen readily on the outer layer of the particle over the timescale expected for typical uninhibited gas-diffusion limited equilibration, resulting in a core-shell structure[24] and kinetically inhibited hygroscopic growth. At very high viscosities, particles may not take up discernible quantities of water vapor over process-relevant timescales except in environments where interfacial free energy is favorable for heterogeneous nucleation.[33]

Atmospheric viscous OA is characterized by molecular species containing large numbers of oxygenated functional groups[34] and with relatively high molecular weight.[17,35,36] Saccharides have similar attributes to these atmospheric components and are commonly used as laboratory proxies for OA.[15,21,37–40] Saccharides are also used widely as excipients and additives in inhalation formulations (e.g. lactose).[41,42] In this work, characteristic condensational timescales are determined for water on various micron-sized aqueous droplets containing a saccharide (sucrose, glucose, raffinose, trehalose) subject to a rapid increase in RH, starting from a RH characteristic of high equilibrium viscosity (10^5 to $>10^{12}$ Pa·s)[43] at temperatures between -7.5 and 20 °C. Under such experimental conditions, droplets could readily undergo condensational growth in the absence of diffusion limitations, whereas growth could be hindered in the presence of such limitations. For comparison, we also present measurements of the condensational kinetics on non-viscous aqueous sodium nitrate particles and aqueous droplets of tetraethylene glycol (henceforth PEG-4).

The condensation kinetics measurements are made using an electrodynamic balance (EDB) to track temporal changes in radius following a rapid increase in RH (<0.5 s) within the trapping

region.[44] Elastic light scattering (intensity with scattering angle) is measured with a time resolution as high as 0.01 s, and the evolving radius and composition are inferred using well-established procedures.[45] An example of the observed change in droplet size is shown in Fig. 1 for the condensation of water on a glucose particle. The timescale (τ) for condensation is characterized by a non-linear least squares fit of the experimental data to the modified Kohlrausch-Williams-Watts (mKWW) equation:[46,47]

$$r(t) = r_f - \left(r_f - r_i\right)e^{-(t/\tau)^{\beta}} \quad (1)$$

where r is the radius of the particle at transition time t, r_i and r_f are the initial and final radii, respectively, and β reflects the departure from a single-exponential fit. The suitability of an equation of this form for modeling the response of a viscous solution droplet to a perturbation in RH has been demonstrated in prior work.[22] Note that while physical interpretations for β have been proposed elsewhere,[48] in this work it was used solely as an empirical stretching parameter.

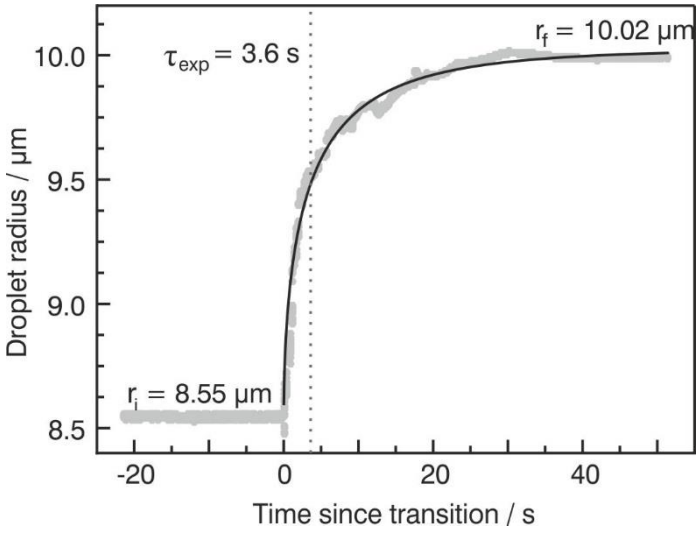

Figure 1. Condensation profile (radius vs. time) for an aqueous glucose droplet (20 °C, RH transition of 25 to 79%): measurement (grey points) and fitted mKWW equation (black curve). Vertical grey dashed line represents $\tau = 3.6$ s.

Reported moisture-dependent viscosities for aqueous solutions of the solutes studied here are summarized in Fig. 2a. Initial viscosities at 20 °C and 25% RH vary from < 1 (for PEG-4/sodium nitrate) to > 10^{10} Pa·s (sucrose). We are not aware of lower temperature viscosity measurements for these compounds, although a model proposed by Rothfuss and Petters suggests sucrose particles at 25% RH have a viscosity well above the 10^{12} Pa·s threshold for the glass transition for all of the temperatures studied here (-7.5, 0 and 20 ºC).[15,20] This is consistent with available literature data for the glass transition of aqueous sucrose solutions, which are summarized in Fig. 2b. Thus, condensation measurements of water on aqueous sucrose particles at an RH ~25% with $T \leq 0$ °C are expected to involve particles initially in a glassy state. As shown in Fig 2b., literature data suggests the RH-induced glass transition for raffinose will occur at ~50% at 0 °C, and ~60% at -7.5 °C, the starting experimental RH values used for raffinose in this work. Thus, we expect raffinose particles at $T \leq 0$ °C to initially have a viscosity at the high end of the semi-solid viscosity range, approaching that of a glass.

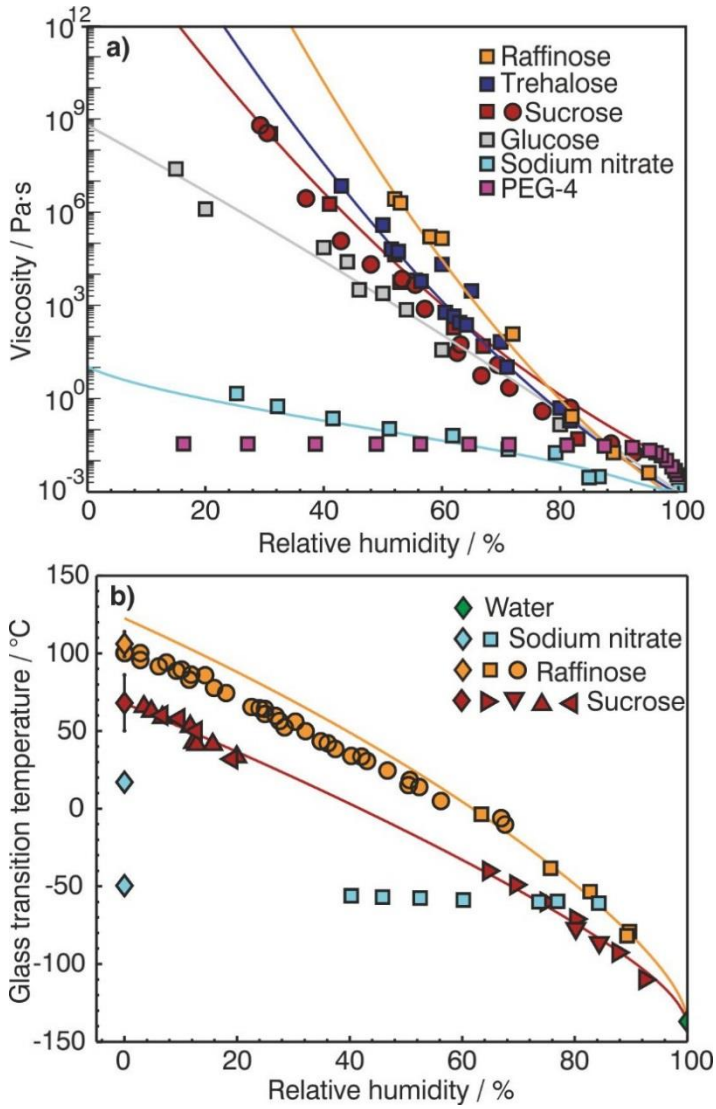

Figure 2. In (a) RH-dependent viscosities of raffinose,[43] trehalose,[43] sucrose,[10,43] glucose,[43] sodium nitrate[49] and PEG4,[50] with polynomial equations from Song et al.[43] for the saccharides and Baldelli et al.[49] for sodium nitrate (solid lines). In (b) experimental RH-dependent glass transition temperatures for binary aqueous solutions of raffinose (yellow squares[16] and circles[51]), sucrose (red triangles,[52] left triangles,[53] right triangles,[54] upside down triangles[55]) and sodium nitrate (blue squares).[56] Pure component glass transition temperatures (diamonds) for raffinose,[15] sucrose,[15] sodium nitrate[57] and water[17] are also reported. Fits to the Gordon-Taylor equation[58] using literature parameters for raffinose[16] and sucrose[15] are indicated by solid lines.

Characteristic time constants for all experiments are summarized in Fig 3a. Most τ values are on the order of 1 s, although a small number (sucrose and raffinose in particular) have values of ~10 s. All measured τ values are within a factor of 15 larger than the fastest system studied – sodium nitrate at 20 °C – and a large majority are within 1 order of magnitude. This similarity exists despite a broad range of initial viscosities, including liquid-like (sodium nitrate and PEG-4 at 20 °C), semi-solid (glucose, trehalose, and raffinose at 20 °C), near-glassy (sucrose at 20 °C and raffinose at colder temperatures) and likely glassy (sucrose < 20 °C). This is further illustrated in Fig 3b, which considers the possible dependency of the τ values on the initial viscosity of the particle. Clearly, systems with low initial viscosity also exhibit the shortest equilibration timescale, although the variation is only marginal. The possible temperature dependence of τ is explored in Fig. 3c. Sodium nitrate has the shortest τ values at all temperatures. In interpreting these results, it is important to remember that all of these systems are hygroscopic. Typical fitted values of the stretching parameter β varied from 0.4 to 1.3, with good reproducibility (±0.1) between identical experimental trials but no obvious systematic pattern.

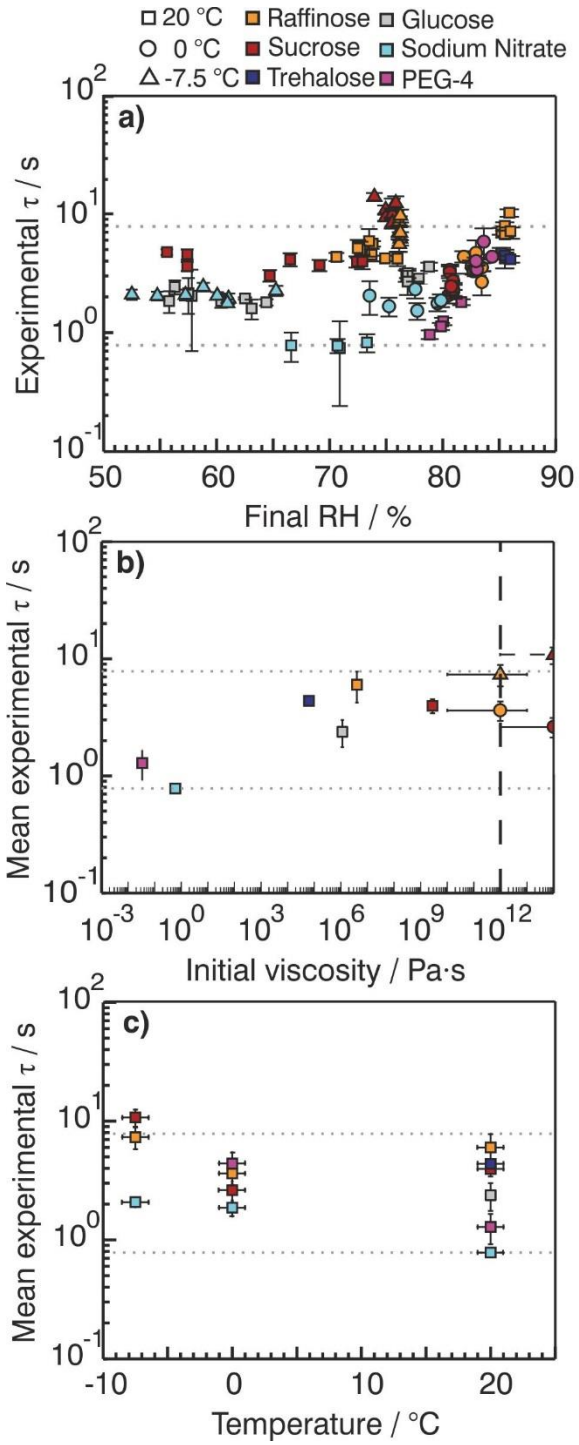

Figure 3. Fitted experimental characteristic condensation times versus (a) final RH, (b) estimated initial viscosity of droplet prior to condensation step, (c) temperature of condensation measurement. Dashed grey horizontal lines delineate the 1-order of magnitude range in τ containing most experimental values. Legend at top for (a)-(c).

In the absence of condensed phase diffusional limitations on growth, droplet size evolution can be modelled using an analytical treatment (first introduced by Kulmala et al.)[59] of the gas diffusional mass flux that accounts for the latent heat of condensation and its impact on the mass transfer rate.[60] Experimental and modelled τ values are compared in Fig 4. Although there is good consistency between experimental and modelled timescales for sodium nitrate, experimental timescales are larger than the modelled timescales for the saccharide droplets, exceeding an order of magnitude in some cases. It should be noted that simulation of water condensation using the Kulmala equation does not account for the time required for the RH change (<0.5 s) in the EDB instrument. The model-observation consistency for sodium nitrate and disparity for the remaining compounds suggests that either bulk diffusion limitations or surface accommodation effects are responsible for the ~1 order of magnitude increase in water uptake timescale in these experiments.

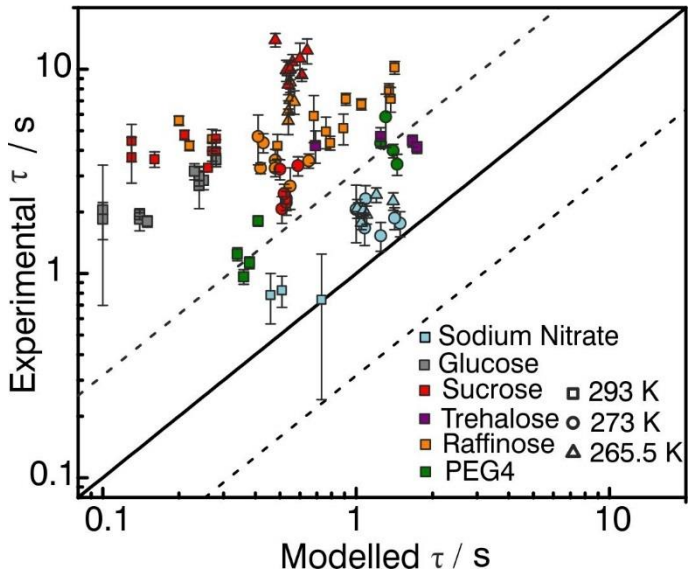

Figure 4. Comparison of fitted experimental and modelled characteristic timescales using the Kulmala equation[59] and mKWW fitting for the experiments performed in this work.

Despite the considerable variation in the range of starting particle viscosities apparent in Fig. 3b (as large as 15 orders of magnitude), the measured timescales for condensational growth and

equilibration of the micron-sized particles following a step increase in RH are typically less than 10 s within one order of magnitude. This viscosity range covers the expected range of relevance for atmospheric OA and for amorphous particles typically used in inhalation therapies. Although these experimental timescales are ~1 order of magnitude longer than timescales predicted using a gas-diffusional condensational growth model for some of the more viscous particles, they are nonetheless significantly shorter than timescales of typical atmospheric processes. For example, at an initial temperature of 20 °C and updraft velocity of 1 m s^{-1}, the timescale to raise the RH from 20 to 80% is 2000 seconds. Under this scenario, even viscous hygroscopic supermicron particles similar to those studied in this work can be expected to effectively track the changing RH, remaining in equilibrium under almost all atmospheric conditions. The most violent supercell thunderstorms, where vertical velocities may approach 50 m s^{-1},[61] would perhaps be an exception. By contrast, highly viscous amorphous particles may require more time to respond to the sudden increase in RH than occurs during a typical inhalation time of 1 s, particularly given that most drug particles start larger than 1 μm in diameter.

Next, we consider the expected radius dependent scaling by calculating bulk mixing times for aqueous sucrose aerosol as a function of radius at 20 °C and variable RH (see Fig. S2). Overall, the calculated bulk mixing and condensational τ values have similar sensitivity to particle size. Assuming experimental timescales decrease along a similar slope with radius, extrapolation would suggest condensational growth occurs on the timescale of milliseconds for 100 nm sucrose particles under ambient atmospheric conditions, fast enough to likely be of limited consequence for atmospheric processes.

We note one key limitation regarding the broad applicability of our results: the systems studied in this work all have liquid-like equilibrium viscosity (< 10 Pa·s) (Fig. 2a) at room temperature

and 78% RH, as might be expected for hygroscopic aerosol where equilibrium water content will be significant. The forcing that drives condensation will invariably lead to plasticization of the particle,[17] which in turn removes the diffusional limitation. In the atmosphere, different chemical compositions and/or colder temperatures will result in particles with much higher equilibrium viscosities, even at high RH. This may be particularly the case if the system is weakly or non-hygroscopic, thus reducing the particle water content and concomitant potentials for plasticization and increases in bulk diffusivity due to the influence of water, even in outer layers of the particle that are likely equilibrated with the ambient environment. The carbohydrates studied in this work contain multiple hydrogen-bonding OH groups, the presence of which are associated with both higher viscosity[34] and greater hygroscopicity.[62] Accordingly, replacement of carbohydrate-carbohydrate hydrogen bonds with carbohydrate-water hydrogen bonds during hygroscopic growth is a plausible plasticization mechanism. This mechanism will be absent for non-hydrogen bonding solutes. In cases where viscosity remains high at the final RH, bulk mixing timescales can be orders of magnitude higher at 10 μm than observed here[21,22] and can remain slow relative to typical timescales of atmospheric processes in which case condensational growth timescales are also slow.[21] Whereas, in the context of inhalation the increased temperature (37 ºC) and very high RH (>99.5 %) water condensation should remain fast. Taken all together, these observations suggest bulk diffusional inhibitions are primarily a concern for condensation onto particles that are weakly (perhaps even non-) hygroscopic in addition to being sufficiently viscous. It should also be recognized that the temperature dependence of hygroscopicity itself is not well resolved but will be a concern if solubility limitations become more pronounced at lower temperatures.

Finally, we have not considered that marginal inhibition in condensational growth rate may arise from a suppressed value of the mass accommodation coefficient (α). Direct measurements of

accommodation coefficients are primarily limited to those for water vapor onto aqueous droplets. Miles et al.[63] suggested a lower limit value of 0.5 for water accommodating onto a water surface, based upon an assessment of five separate methods for measuring accommodation coefficients. This limit was shown to be consistent with subsequent measurements made by Davies et al.[64] using the same instrument as employed here. This would suggest that even assuming a conservative lower bound, the value of α would need to be about a factor of 40 smaller than this limiting value of 0.5 (Fig. S3). This augurs that accommodation will not be limiting, at least once the condensation process has begun and an aqueous shell at high water activity is present on the droplet surface. Surface accommodation inhibition may be of greater concern in systems less hygroscopic than studied in this work, due to their more hydrophobic nature.

In summary, water condensation timescales on hygroscopic amorphous glassy particles are less than 10 s under the conditions of high RH and there is only a marginal dependence on the starting viscosity of the particle. Although these measurements suggest timescales for water condensation can be expected to be short, weakly or non-hygroscopic aerosol particularly at low temperatures may lengthen timescales of water condensation.

EXPERIMENTAL METHODS

The theory and operation of the EDB have been discussed extensively in prior work[44,65] and full details of its application in this work are provided in the SI. The EDB chamber RH within the EDB chamber were determined from probe droplet measurements.[65] For each experiment, the initial equilibrium radius (r_i) at low RH was calculated as the mean of the measured radii across a time window of 1 s prior to the condensation step. Once r_i was fixed, r_f, τ, and β were calculated via an unbounded fit to Eq. (1) as described above.

The gas diffusional growth model first introduced by Kulmala and coworkers[59] has been described extensively in previous publications and details are provided in the SI.[44,60,65] Simulations of time dependent growth were performed using values of temperature, initial and final RHs, and initial particle size identical to those for each EDB experiment. For comparison to experimental measurements, modeled characteristic time constants were calculated by fitting these data to Eq. (1), fixing r_i to the first simulated radius.

ASSOCIATED CONTENT

Supporting Information

The supporting information contains two additional figures illustrating modelling of experimental and simulated condensation curves. A description of the EDB technique and experimental procedure is provided. Additionally, the gas-phase diffusional growth modelling and the bulk mixing timescale modelling are described.

AUTHOR INFORMATION

ORCID IDs: Nicholas E. Rothfuss: 0000-0002-1495-1902, Aleksandra Marsh: 0000-0002-0480-786, Grazia Rovelli: 0000-0001-9454-3169, Markus D. Petters: 0000-0002-4082-1693, Jonathan P. Reid: 0000-0001-6022-1778

Notes

The authors declare no competing financial interests.

ACKNOWLEDGMENT

This work was primarily supported by the United Kingdom Natural Environment Research Council International Opportunities Fund award NE/N006801/1. NER and MDP acknowledge additional support by the United States Department of Energy, Office of Science, Biological and Environmental Research grant number DE-SC0012043. AM thanks EPSRC for support through

the Doctoral Training Award. We wish to thank Allen Haddrell for assistance with the EDB. The experimental data presented in each figure is provided through the University of Bristol data repository (DOI:10.5523/bris.6a34adi090bo27ds5kkm5y9h5).

REFERENCES

(1) Haddrell, A. E.; Davies, J. F.; Reid, J. P. Dynamics of Particle Size on Inhalation of Environmental Aerosol and Impact on Deposition Fraction. *Environ. Sci. Technol.* **2015**, *49*, 14512–14521.

(2) Vehring, R.; Foss, W. R.; Lechuga-Ballesteros, D. Particle Formation in Spray Drying. *Aerosol Sci.* **2007**, *38*, 728–746.

(3) Vehring, R. Pharmaceutical Particle Engineering via Spray Drying. *Pharm. Res.* **2008**, *25*, 999–1022.

(4) Davies, J. F.; Haddrell, A. E.; Miles, R. E. H.; Bull, C. R.; Reid, J. P. Bulk, Surface, and Gas-Phase Limited Water Transport in Aerosol. *J. Phys. Chem. A* **2012**, *116*, 10987–10998.

(5) Berkemeier, T.; Huisman, A. J.; Ammann, M.; Shiraiwa, M.; Koop, T.; Pöschl, U. Kinetic Regimes and Limiting Cases of Gas Uptake and Heterogeneous Reactions in Atmospheric Aerosols and Clouds: A General Classification Scheme. *Atmos. Chem. Phys.* **2013**, *13*, 6663–6686.

(6) O'Meara, S.; Topping, D. O.; McFiggans, G. The Rate of Equilibration of Viscous Aerosol Particles. *Atmos. Chem. Phys.* **2016**, *16*, 5299–5313.

(7) Pajunoja, A.; Lambe, A. T.; Hakala, J. Adsorptive Uptake of Water by Semisolid Secondary

Aerosols. *Geophys. Res. Lett.* **2015**, *42*, 3063–3068.

(8) Reid, J. P.; Bertram, A. K.; Topping, D. O.; Laskin, A.; Martin, S. T.; Petters, M. D.; Pope, F. D.; Rovelli, G. The Viscosity of Atmospherically Relevant Organic Particles. *Nat. Commun.* **2018**, *9*, 956.

(9) Renbaum-Wolff, L.; Grayson, J. W.; Bateman, A. P.; Kuwata, M.; Sellier, M.; Murray, B. J.; Shilling, J. E.; Martin, S. T.; Bertram, A. K. Viscosity of α-Pinene Secondary Organic Material and Implications for Particle Growth and Reactivity. *Proc. Natl. Acad. Sci. U. S. A.* **2013**, *110*, 8014–8019.

(10) Power, R. M.; Simpson, S. H.; Reid, J. P.; Hudson, A. J. The Transition from Liquid to Solid-like Behaviour in Ultrahigh Viscosity Aerosol Particles. *Chem. Sci.* **2013**, *4*, 2597–2604.

(11) Song, M.; Liu, P. F.; Hanna, S. J.; Li, Y. J.; Martin, S. T.; Bertram, A. K. Relative Humidity-Dependent Viscosities of Isoprene-Derived Secondary Organic Material and Atmospheric Implications for Isoprene-Dominant Forests. *Atmos. Chem. Phys.* **2015**, *15*, 5145–5159.

(12) Song, M.; Liu, P. F.; Hanna, S. J.; Zaveri, R. A.; Potter, K.; You, Y.; Martin, S. T.; Bertram, A. K. Relative-Humidity Dependent Viscosity of Secondary Organic Material from Toluene Photo-Oxidation and Possible Implications for Organic Particulate Matter over Megacities. *Atmos. Chem. Phys.* **2016**, *16*, 8817–8830.

(13) Zhang, Y.; Sanchez, M. S.; Douet, C.; Wang, Y.; Bateman, A. P.; Gong, Z.; Kuwata, M.; Renbaum-Wolff, L.; Sato, B. B.; Liu, P. F.; et al. Changing Shapes and Implied Viscosities of Suspended Submicron Particles. *Atmos. Chem. Phys.* **2015**, *15*, 7819–7829.

(14) Järvinen, E.; Ignatius, K.; Nichman, L.; Kristensen, T. B.; Fuchs, C.; Höppel, N.; Corbin, J. C.; Craven, J.; Duplissy, J.; Ehrhart, S.; et al. Observation of Viscosity Transition in α-Pinene Secondary Organic Aerosol. *Atmos. Chem. Phys.* **2016**, *16*, 4423–4438.

(15) Rothfuss, N. E.; Petters, M. D. Characterization of the Temperature and Humidity-Dependent Phase Diagram of Amorphous Nanoscale Organic Aerosols. *Phys. Chem. Chem. Phys.* **2017**.

(16) Zobrist, B.; Marcolli, C.; Pedernera, D. A.; Koop, T. Do Atmospheric Aerosols Form Glasses? *Atmos. Chem. Phys.* **2008**, *8*, 5221–5244.

(17) Koop, T.; Bookhold, J.; Shiraiwa, M.; Pöschl, U. Glass Transition and Phase State of Organic Compounds: Dependency on Molecular Properties and Implications for Secondary Organic Aerosols in the Atmosphere. *Phys. Chem. Chem. Phys.* **2011**, *13*, 19238–19255.

(18) Mikhailov, E.; Vlasenko, S.; Martin, S. T.; Koop, T.; Pöschl, U. Amorphous and Crystalline Aerosol Particles Interacting with Water Vapor: Conceptual Framework and Experimental Evidence for Restructuring, Phase Transitions and Kinetic Limitations. *Atmos. Chem. Phys.* **2009**, *9*, 9491–9522.

(19) Virtanen, A.; Joutsensaari, J.; Koop, T.; Kannosto, J.; Yli-Pirilä, P.; Leskinen, J.; Mäkelä, J. M.; Holopainen, J. K.; Pöschl, U.; Kulmala, M.; et al. An Amorphous Solid State of Biogenic Secondary Organic Aerosol Particles. *Nature* **2010**, *467*, 824–827.

(20) Debenedetti, P. G.; Stillinger, F. H. Supercooled Liquids and the Glass Transition. *Nature* **2001**, *410*, 259–267.

(21) Bones, D. L.; Reid, J. P.; Lienhard, D. M.; Krieger, U. K. Comparing the Mechanism of

Water Condensation and Evaporation in Glassy Aerosol. *Proc. Natl. Acad. Sci. U. S. A.* **2012**, *109*, 11613–11618.

(22) Rickards, A. M.; Song, Y.-C.; Miles, R. E. H.; Preston, T. C.; Reid, J. P. Variabilities and Uncertainties in Characterising Water Transport Kinetics in Glassy and Ultraviscous Aerosol. *Phys. Chem. Chem. Phys.* **2015**, *17*, 10059–10073.

(23) Robinson, C. B.; Schill, G. P.; Tolbert, M. a. Optical Growth of Highly Viscous Organic/Sulfate Particles. *J. Atmos. Chem.* **2014**, *71*, 145–156.

(24) Berkemeier, T.; Shiraiwa, M.; Pöschl, U.; Koop, T. Competition between Water Uptake and Ice Nucleation by Glassy Organic Aerosol Particles. *Atmos. Chem. Phys.* **2014**, *14*, 12513–12531.

(25) Mikhailov, E.; Vlasenko, S.; Rose, D.; Pöschl, U. Mass-Based Hygroscopicity Parameter Interaction Model and Measurement of Atmospheric Aerosol Water Uptake. *Atmos. Chem. Phys.* **2013**, *13*, 717–740.

(26) Zobrist, B.; Soonsin, V.; Luo, B. P.; Krieger, U. K.; Marcolli, C.; Peter, T.; Koop, T. Ultra-Slow Water Diffusion in Aqueous Sucrose Glasses. *Phys. Chem. Chem. Phys.* **2011**, *13*, 3514–3526.

(27) Shiraiwa, M.; Pfrang, C.; Koop, T.; Pöschl, U. Kinetic Multi-Layer Model of Gas-Particle Interactions in Aerosols and Clouds (KM-GAP): Linking Condensation, Evaporation and Chemical Reactions of Organics, Oxidants and Water. *Atmos. Chem. Phys.* **2012**, *12*, 2777–2794.

(28) Price, H. C.; Murray, B. J.; Mattsson, J.; O'Sullivan, D.; Wilson, T. W.; Baustian, K. J.;

Benning, L. G. Quantifying Water Diffusion in High-Viscosity and Glassy Aqueous Solutions Using a Raman Isotope Tracer Method. *Atmos. Chem. Phys.* **2014**, *14*, 3817–3830.

(29) Marshall, F. H.; Miles, R. E. H.; Song, Y.; Ohm, P. B.; Power, R. M.; Reid, J. P.; Dutcher, C. S. SUPPLEMENTARY Diffusion and Reactivity in Ultraviscous Aerosol and the Correlation with Particle Viscosity. *Chem. Sci.* **2016**, *7*, 1298–1308.

(30) Lu, J. W.; Rickards, A. M. J.; Walker, J. S.; Knox, K. J.; Miles, R. E. H.; Reid, J. P.; Signorell, R. Timescales of Water Transport in Viscous Aerosol: Measurements on Sub-Micron Particles and Dependence on Conditioning History. *Phys. Chem. Chem. Phys.* **2014**, *16*, 9819–9830.

(31) Bastelberger, S.; Krieger, U. K.; Luo, B.; Peter, T. Diffusivity Measurements of Volatile Organics in Levitated Viscous Aerosol Particles. *Atmos. Chem. Phys.* **2017**, 8453–8471.

(32) Chenyakin, Y.; Ullmann, D. A.; Evoy, E.; Renbaum-Wolff, L.; Kamal, S.; Bertram, A. K. Diffusion Coefficients of Organic Molecules in Sucrose – Water Solutions and Comparison with Stokes – Einstein Predictions. *Atmos. Chem. Phys.* **2017**, *17*, 2423–2435.

(33) Fletcher, N. H. Size Effect in Heterogeneous Nucleation. *J. Chem. Phys.* **1958**, *29*, 572–576.

(34) Rothfuss, N. E.; Petters, M. D. Influence of Functional Groups on the Viscosity of Organic Aerosol. *Environ. Sci. Technol.* **2017**, *51*, 271–279.

(35) Hinks, M. L.; Brady, M. V; Lignell, H.; Song, M.; Grayson, J. W.; Bertram, A.; Lin, P.; Laskin, A.; Laskin, J.; Nizkorodov, S. a. Effect of Viscosity on Photodegradation Rates in

Complex Secondary Organic Aerosol Materials. *Phys. Chem. Chem. Phys.* **2016**, *18*, 8785–8793.

(36) DeRieux, W.-S. W.; Li, Y.; Lin, P.; Laskin, J.; Laskin, A.; Bertram, A. K.; Nizkorodov, S. A.; Shiraiwa, M. Predicting the Glass Transition Temperature and Viscosity of Secondary Organic Material Using Molecular Composition. *Atmos. Chem. Phys.* **2018**, *18*, 6331–6351.

(37) Lienhard, D. M.; Huisman, A. J.; Krieger, U. K.; Rudich, Y.; Marcolli, C.; Luo, B. P.; Bones, D. L.; Reid, J. P.; Lambe, A. T.; Canagaratna, M. R.; et al. Viscous Organic Aerosol Particles in the Upper Troposphere: Diffusivity-Controlled Water Uptake and Ice Nucleation? *Atmos. Chem. Phys.* **2015**, *15*, 13599–13613.

(38) Baustian, K. J.; Wise, M. E.; Jensen, E. J.; Schill, G. P.; Freedman, M. A.; Tolbert, M. A. State Transformations and Ice Nucleation in Amorphous (Semi-)Solid Organic Aerosol. *Atmos. Chem. Phys.* **2013**, *13*, 5615–5628.

(39) Petters, S. S.; Petters, M. D. Surfactant Effect on Cloud Condensation Nuclei for Two-Component Internally Mixed Aerosols. *J. Geophys. Res. Atmos.* **2016**, *121*, 1878–1895.

(40) Price, H. C.; Mattsson, J.; Murray, B. J. Sucrose Diffusion in Aqueous Solution. *Phys. Chem. Chem. Phys.* **2016**, *18*, 19207–19216.

(41) Pilcer, G.; Amighi, K. Formulation Strategy and Use of Excipients in Pulmonary Drug Delivery. *Int. J. Pharm.* **2010**, *392*, 1–19.

(42) Chow, A. H. L.; Tong, H. H. Y.; Chattopadhyay, P.; Shekunov, B. Y. Particle Engineering for Pulmonary Drug Delivery. *Pharm. Res.* **2007**, *24*, 411–437.

(43) Song, Y. C.; Haddrell, A. E.; Bzdek, B. R.; Reid, J. P.; Bannan, T.; Topping, D. O.; Percival,

C.; Cai, C. Measurements and Predictions of Binary Component Aerosol Particle Viscosity. *J. Phys. Chem. A* **2016**, No. 41, 8123–8137.

(44) Davies, J. F.; Haddrell, A. E.; Rickards, A. M. J.; Reid, J. P. Simultaneous Analysis of the Equilibrium Hygroscopicity and Water Transport Kinetics of Liquid Aerosol. *Anal. Chem.* **2013**, *85*, 5819–5826.

(45) Marsh, A.; Miles, R. E. H.; Rovelli, G.; Cowling, A. G.; Nandy, L.; Dutcher, C. S.; Reid, J. P. SUPPORTING Influence of Organic Compound Functionality on Aerosol Hygroscopicity: Dicarboxylic Acids, Alkyl-Substituents, Sugars and Amino Acids. *Atmos. Chem. Phys.* **2017**, *17*, 5583–5599.

(46) Williams, G.; Watts, D. C. Non-Symmetrical Dielectric Relaxation Behaviour Arising from a Simple Empirical Decay Function. *Trans. Faraday Soc.* **1970**, *66*, 80–85.

(47) Kohlrausch, R. Theorie Des Elektrischen Rückstandes in Der Leidener Flasche. *Ann. Phys.* **1854**, *167*, 179–214.

(48) Ingram, S.; Cai, C.; Song, Y.-C.; Glowacki, D. R.; Topping, D. O.; O'Meara, S.; Reid, J. P. Characterising the Evaporation Kinetics of Water and Semi-Volatile Organic Compounds from Viscous Multicomponent Organic Aerosol Particles. *Phys. Chem. Chem. Phys.* **2017**, *19*, 31634–31646.

(49) Baldelli, A.; Power, R. M.; Miles, R. E. H.; Reid, J. P.; Vehring, R. Effect of Crystallization Kinetics on the Properties of Spray Dried Microparticles. *Aerosol Sci. Technol.* **2016**, *50*, 693–704.

(50) Begum, S. K.; Clarke, R. J.; Ahmed, M. S.; Begum, S.; Saleh, M. a. Volumetric,

Viscosimetric and Surface Properties of Aqueous Solutions of Triethylene Glycol, Tetraethylene Glycol, and Tetraethylene Glycol Dimethyl Ether. *J. Mol. Liq.* **2013**, *177*, 11–18.

(51) Kajiwara, K.; Franks, F. Crystalline and Amorphous Phases in the Binary System Water – Raffinose. *J. Chem. Soc. Faraday Trans.* **1997**, *93*, 1779–1783.

(52) Elamin, A. A.; Sebhatu, T.; Ahlneck, C. The Use of Amorphous Model Substances to Study Mechanically Activated Materials in the Solid State. *Int. J. Pharm.* **1995**, *119*, 25–36.

(53) Saleki-Gerhardt, A.; Zografi, G. Non-Isothermal and Isothermal Crystallization of Sucrose from the Amorphous State. *Pharm. Res.* **1994**, *11*, 1166–1173.

(54) Luyet, B.; Rasmussen, D. Study by Differential Thermal Analysis of the Temperatures of Instability of Rapidly Cooled Solutions of Glycerol, Ethylene Glycol, Sucrose and Glucose. *Biodynamica* **1968**, *10*, 167–191.

(55) Jansson, H.; Bergman, R.; Swenson, J. Dynamics of Sugar Solutions as Studied by Dielectric Spectroscopy. *J. Non. Cryst. Solids* **2005**, *351*, 2858–2863.

(56) Angell, C. A.; Helphrey, D. B. Corresponding States and the Glass Transition for Alkali Metal Nitrates. *J. Phys. Chem.* **1971**, *75*, 2306–2312.

(57) Dette, H. P.; Koop, T. Glass Formation Processes in Mixed Inorganic/Organic Aerosol Particles. *J. Phys. Chem. A* **2015**, *119*, 4552–4561.

(58) Gordon, M.; Taylor, J. S. Ideal Copolymers and the Second-Order Transitions of Synthetic Rubbers. I. Non-Crystalline Copolymers. *J. Appl. Chem.* **1952**, *2*, 493–500.

(59) Kulmala, M.; Vesala, T.; Wagner, P. E. An Analytical Expression For the Rate of Binary Condensational Particle Growth. *Proc. R. Soc. A Math. Phys. Eng. Sci.* **1993**, *441*, 589–605.

(60) Kulmala, M.; Vesala, T.; Wagner, P. E. An Analytical Expression for the Rate of Binary Condensational Particle Growth. *Proc. R. Soc. London A Math. Phys. Sci.* **1993**, *441*, 589–605.

(61) Marshall, T. C.; Rust, W. D.; Stolzenburg, M. Electrical Structure and Updraft Speeds in Thunderstorms over the Southern Great Plains. *J. Geophys. Res. Atmos.* **1995**, *100*, 1001–1015.

(62) Suda, S. R.; Petters, M. D.; Yeh, G. K.; Strollo, C.; Matsunaga, A.; Faulhaber, A.; Ziemann, P. J.; Carrico, C. M.; Prenni, A. J.; Sullivan, R. C.; et al. The Influence of Functional Groups on Organic Aerosol Cloud Condensation Nuclei Activity. *Environ. Sci. Technol.* **2014**, *48*, 10182–10190.

(63) Miles, R. E. H.; Reid, J. P.; Riipinen, I. Comparison of Approaches for Measuring the Mass Accommodation Coefficient for the Condensation of Water and Sensitivities to Uncertainties in Thermophysical Properties. *J. Phys. Chem. A* **2012**, *116*, 10810–10825.

(64) Davies, J. F.; Miles, R. E. H.; Haddrell, A. E.; Reid, J. P. Temperature Dependence of the Vapor Pressure and Evaporation Coefficient of Supercooled Water. *J. Geophys. Res.* **2014**, *119*, 10931–10940.

(65) Rovelli, G.; Miles, R. E. H.; Reid, J. P.; Clegg, S. L. Accurate Measurements of Aerosol Hygroscopic Growth over a Wide Range in Relative Humidity. *J. Phys. Chem. A* **2016**, *120*, 4376–4388.